JGR Atmospheres

RESEARCH ARTICLE
10.1029/2021JD035888

Key Points:

- Glacier was melting at a rate of 0.32 ± 0.007 m w.e./yr during 1982–2011, and it accelerated with a rate of 0.42 mm/yr
- Glacier and snow melt contributed 17.6% of total annual discharge during 1982–2011; it would decrease to 11.9% during 2021–2050 under RCP8.5
- Longwave radiation, air temperature, humidity and wind determined glacier melt trend, and shortwave radiation impacted melt rate fluctuation

Supporting Information:

Supporting Information may be found in the online version of this article.

Correspondence to:

L. Feng,
fengl@sustech.edu.cn

Citation:

Qi, W., Feng, L., Kuang, X., Zheng, C., Liu, J., Chen, D., et al. (2022). Divergent and changing importance of glaciers and snow as natural water reservoirs in the eastern and southern Tibetan Plateau. *Journal of Geophysical Research: Atmospheres*, *127*, e2021JD035888. https://doi.org/10.1029/2021JD035888

Received 17 SEP 2021
Accepted 19 MAR 2022

Divergent and Changing Importance of Glaciers and Snow as Natural Water Reservoirs in the Eastern and Southern Tibetan Plateau

Wei Qi[1], Lian Feng[1], Xingxing Kuang[1], Chunmiao Zheng[1], Junguo Liu[1], Deliang Chen[2], Yong Tian[1], and Yingying Yao[3]

[1]School of Environmental Science and Engineering, Southern University of Science and Technology, Shenzhen, China, [2]Regional Climate Group, Department of Earth Sciences, University of Gothenburg, Gothenburg, Sweden, [3]Department of Earth and Environmental Science, School of Human Settlements and Civil Engineering, Xi'an Jiaotong University, Xi'an, China

Abstract Glaciers and snow are natural water reservoirs in the Tibetan Plateau (TP), affecting ecosystems, water and food security, and more than one billion downstream people. Meltwater volumes are traditionally estimated using the degree-day concept considering only air temperature, which cannot consider the influence from downward solar and longwave radiation, humidity, wind and resultant turbulent heat fluxes. Here, we used a physically based energy budget approach considering the full energy balance in seven large river basins in the eastern and southern TP. For 1982–2011, the estimated average glacier melt was 0.32 ± 0.007 m water equivalent/yr with large spatial variability. Air temperature, downward longwave radiation, humidity, and wind speed influenced the overall glacier melt trend, and glacier melt accelerated with a rate of 0.42 mm/yr. Yet, downward shortwave radiation played an additional role in influencing the glacier melt rate fluctuation. On average, snow and glacier melt contributed 17.6% of annual river discharge during 1982–2011, including 10.0% from snow and 7.6% from glaciers. The highest and lowest relative melt contributions were in the Yarlung Tsangpo and Yalong Rivers, respectively. Mainly due to decreasing snow melt, glacier and snow melt contributions to discharge would decrease to 11.9% during 2021–2050 under the extreme climate scenario (RCP8.5), and the greatest change in the relative contributions would occur in the Upper Nu River (−9.2%). These findings indicate the divergent and changing importance of glaciers and snow as natural water reservoirs, potentially affecting socioeconomic development and adaptation to climate change in South, Southeast, and East Asia.

1. Introduction

Glaciers and seasonal snow are important water storage for regional water cycle, altering the seasonality of the downstream water resources (Hugonnet et al., 2021; Mölg et al., 2014; Zemp et al., 2019). The Tibetan Plateau (TP) has the largest glacier volume on earth, except for the South and North Poles, and plays an important role in the hydrological cycle (Yao et al., 2019). The eastern and southern TP is the source regions of several large Asian rivers, including the Yangtze, Yellow, Lancang-Mekong, Nu-Salween, and Yarlung Tsangpo-Brahmaputra Rivers (Immerzeel & Bierkens, 2012; Immerzeel et al., 2010). The meltwater from snow and glaciers has a remarkable influence on downstream food security, ecosystems, water security, flood disasters, and hydropower production in South, Southeast, and East Asia, affecting a total population exceeding one billion (Bolch et al., 2012; Immerzeel et al., 2020; Nie et al., 2021; T. Wang et al., 2021).

Many previous modeling studies were based on the degree-day approach to study glacier and snow melt contributions to discharge in the eastern and southern TP. The modeling studies have been carried out in the Upper Yangtze, Upper Yellow, Upper Lancang, Upper Nu, and Yarlung Tsangpo Rivers, and so on (Chen et al., 2017; Han et al., 2019; Lutz et al., 2014; L. Zhang et al., 2013; Y. Zhang et al., 2019). Although the degree-day approach was commonly utilized, it is an empirical model considering the impact of air temperature through an empirical relationship between melt and the degree-day, and cannot accurately reflect the energy budget on glaciers (Azam et al., 2021; Litt et al., 2019; Milly et al., 2020; Sicart et al., 2008). Considerations of the full energy balance of glacier and snow melt in hydrological modeling in the whole of eastern and southern TP remains limited so far. Without considering the full energy balance, the influence of downward radiation on the glacier melt trend and melt rate fluctuation is not well understood. In addition, the spatial distribution of snow and glacier melt

contributions to total discharge, and acceleration rate of glacier melt remains unknown in the whole of eastern and southern TP.

Considering downward radiation could improve glacier and snow melt estimation. Downward shortwave radiation and longwave radiation could induce remarkable changes in glacier melt rates (Huss & Bauder, 2009; Huss et al., 2009; Litt et al., 2019; Marzeion et al., 2020; Miles et al., 2018; Thibert et al., 2018), and could even play more important roles than air temperature (Sicart et al., 2008). In addition, downward radiation could have a large influence on the spatial distribution of glacier melt (Vincent & Six, 2013). In the west TP, the downward shortwave radiation is the largest energy source controlling the temporal variability of glacier melt (Azam et al., 2021, 2014; Datt et al., 2008). In the eastern and southern TP, debris cover is much less than it is in other parts of the TP (Scherler et al., 2011), and the influence of solar radiation on glacier melt would be stronger, because solar radiation influences debris free glaciers more than debris-covered glaciers (Wijngaard et al., 2019). In the eastern and southern TP, the question is how the downward radiation influences the glacier melt trends and melt rate fluctuations.

In this study, we quantified glacier and snow melt contributions to runoff/discharge in the whole of eastern and southern TP using a physically-based water and energy budget model, in which the full energy budgets were considered. Based on the model simulation, the influence of downward shortwave and longwave radiation, air temperature, and other climate variables on glacier melt was analyzed, the acceleration rate of glacier melt was quantified, and the spatial distribution of snow and glacier melt contributions to total discharge was studied. We examined seven large river basins in the eastern and southern TP in a historical period and a near-future period under the extreme climate scenario, that is, Representative Concentration Pathway (RCP) 8.5 scenario. The river basins included the Yarlung Tsangpo, Upper Nu, Upper Lancang, Upper Yangtze, Yalong, Min and Upper Yellow River Basins. The results provide critical information on the importance of glaciers and snow as natural water reservoirs to sustain freshwater supplies for people and ecosystems.

2. Methodology

2.1. The Study Region

The total area (total glacier area) of the river basins in this study is 1.09 million km^2 (9,240 km^2; Figure 1a and Table 1; Farinotti et al., 2019; RGI Consortium, 2017), and the mean elevation is 4,143 m. The Yarlung Tsangpo, Upper Yangtze, and Upper Nu River Basins have more glaciers than that in the other river basins, and the Yalong River Basin has the lowest glacier area among the basins in this study.

2.2. The Data Sets

Downward shortwave and longwave radiation, specific humidity, wind speed, and air temperature data were from the China Meteorological Forcing Data set (CMFD), which has a spatial resolution of 0.1 degrees and was developed by the Institute of Tibetan Plateau Research, Chinese Academy of Sciences based on China's meteorological station data. The development and evaluations of the CMFD data have been detailed in the previous study by He et al. (2020). The China Gauge-based Daily Precipitation Analysis (CGDPA) data were used in this study, which were generated by the National Meteorological Information Center of China using ~2,400 precipitation gauges (Shen & Xiong, 2016; Zhao & Zhu, 2015). The CGDPA precipitation has been successfully used in the TP for hydrological studies, for example, Chen et al. (2017), Han et al. (2019), and X. Li et al. (2019), and therefore we also used the CGDPA precipitation. The development and evaluations of the CGDPA precipitation data have been detailed in the previous study by Shen and Xiong (2016). All the forcing data were regridded into 0.1 degree cells, and the resolution is acceptable for the hydrological modeling considering that the study region is large (Pritchard, 2019; T. Wang et al., 2021). The data from 1982 to 2011 (30 yr) were used in this study. The Gravity Recovery and Climate Experiment (GRACE) data were used in evaluations of total water storage changes (TWSCs), and the data were collected from https://grace.jpl.nasa.gov/data/get-data/jpl_global_mascons/. Moderate Resolution Imaging Spectroradiometer (MODIS) snow cover data were used in snow cover fraction evaluations. Glacial debris cover information was from the study by Herreid and Pellicciotti (2020), and is based on the Randolph Glacier Inventory (RGI) 6.0 database (RGI Consortium, 2017), which is the same to the data we used and therefore is consistent with our model simulation. More details about the data sets used in this study can be found in Supporting Information S1.

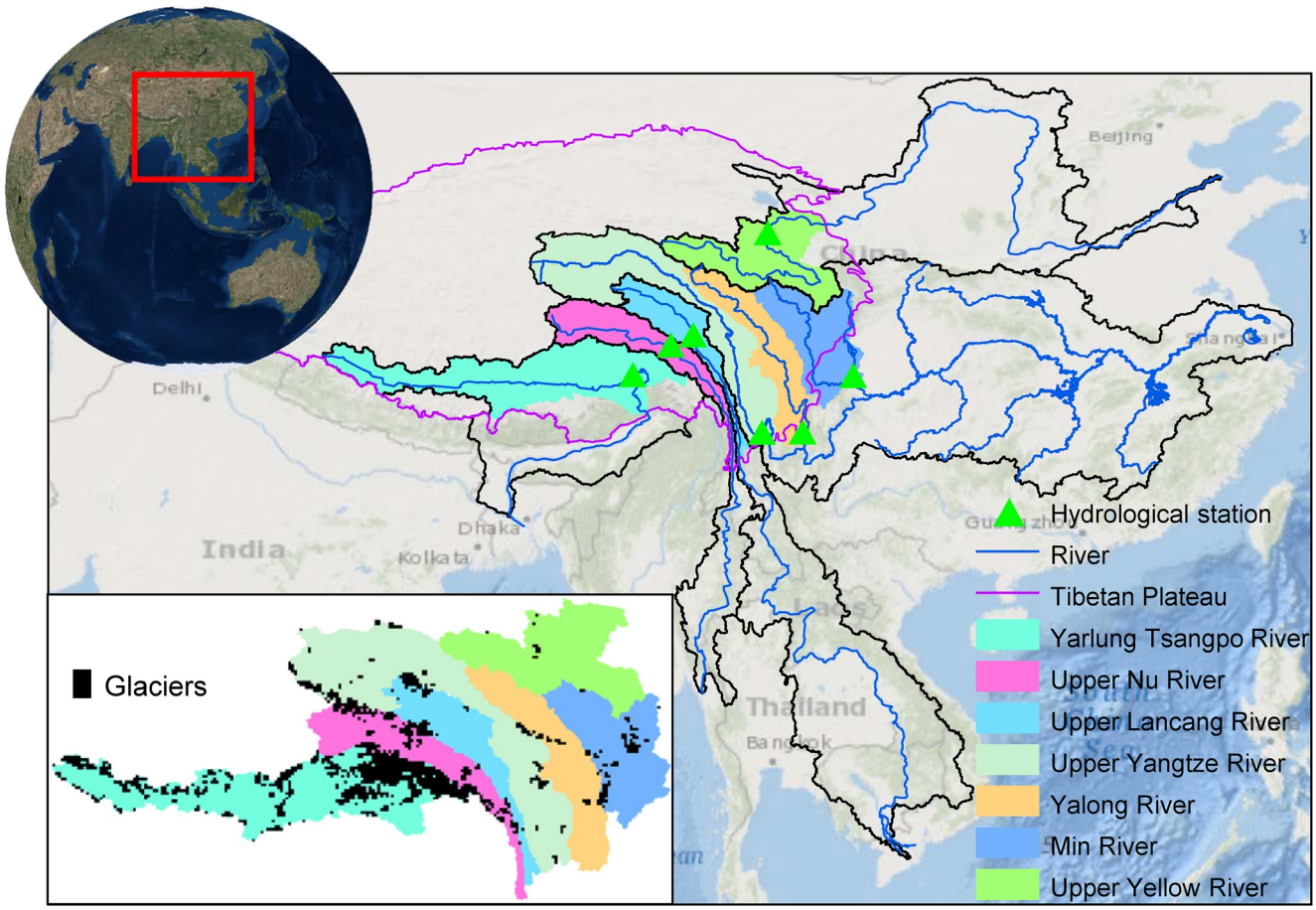

Figure 1. The study region.

For future period (starts from 2021 in this study), climate data from the Inter-Sectoral Impact Model Intercomparison Project (ISIMIP2b) were used (Frieler et al., 2017). ISIMIP2b data provide four global circulation model simulations on a daily scale (Frieler et al., 2017; Lange, 2016, 2018), that is, GFDL-ESM2M, HadGEM2-ES, IPSL-CM5A-LR, and MIROC5. The climate data include precipitation, air temperature, downward longwave radiation, downward shortwave radiation, wind speed, air pressure, and specific humidity. The leaf area index for future periods was from ISIMIP2b and simulated by the Community Land Model (Lawrence et al., 2011; Thiery

Table 1
Details of the River Basins Studied

Basin	Basin area (km^2)	Mean elevation (m)	Mean annual precipitation (mm)	Hydrological gauge used	Glacier area (km^2)	Percentage of glacier (debris) area
Yarlung Tsangpo River	256,864 (204,450, 79.6%)	4,627	550	Nuxia	6,559(2,639, 40.2%)	2.6% (6.7%)
Upper Nu River	112,108 (72,893, 65.0%)	4,550	640	Jiayuqiao	925(625, 67.6%)	0.8% (4.2%)
Upper Lancang River	86,797 (53,713, 61.9%)	4,347	656	Changdu	254(201, 79.1%)	0.3% (2.5%)
Upper Yangtze River	238,742 (215,600, 90.3%)	4,449	557	Shigu	1,046(1,036, 99.0%)	0.4% (1.2%)
Yalong River	116,600	3,957	799	Ertan	54	0.05% (0.0%)
Min River	125,980	3,096	912	Wutongqiao	297	0.2% (0.0%)
Upper Yellow River	148,164	3,974	473	Tangnaihai	105	0.07% (0.0%)

Note. The "Basin area" and "Glacier area" in the brackets are the area and corresponding percentage controlled by the hydrological gauges when the hydrological gauges are not located in the outlets of the entire river basins. The glacier data are from Farinotti et al. (2019) and the Randolph Glacier Inventory (RGI) version 6.0 data set (RGI Consortium, 2017). The debris cover percentages represent the percentages of the total glacier area.

et al., 2017). By using these future climate data, the influence from precipitation, temperature, radiation, humidity, and wind were considered together in the snow and glacier melt study. The bias corrections for ISIMIP2b data were carried out by the ISIMIP team (https://www.isimip.org/gettingstarted/isimip2b-bias-correction/; see the Supporting Information S1 for more details). ISIMIP2b has been commonly used in hydrology-related studies globally (e.g., Gernaat et al., 2021; Gudmundsson et al., 2021; Woolway et al., 2021). The initial glacier thickness data were from the study by Farinotti et al. (2019), which was based on the RGI 6.0 database (RGI Consortium, 2017). The nonparametric Mann-Kendall analysis approach was used to analyze the significance of the changing trends at a significance level of 0.05 (Kendall, 1975; Mann, 1945).

2.3. The WEB-DHM-S Model and Analysis Method

The water and energy budget-based distributed biosphere hydrological model with improved snow physics (WEB-DHM-S; Qi et al., 2022; Shrestha et al., 2010; L. Wang, Koike, Yang, & Yang, 2009; L. Wang, Koike, Yang, Jackson, et al., 2009; L. Wang et al., 2017) was used in this study. The WEB-DHM-S combines the simple biosphere scheme (SiB2) land surface model, a hydrological model based on geomorphology developed by D. Yang (1998), and a physically based snowmelt model (Shrestha et al., 2010; L. Wang, Koike, Yang, & Yang, 2009; L. Wang, Koike, Yang, & Yeh, 2009; L. Wang et al., 2017). In WEB-DHM-S, the influence of radiation, temperature, humidity, wind, and precipitation on snow and glacier melt are considered in a physical way (Shrestha et al., 2015). The snow compaction process, and the accumulation and melt of snow falling on glaciers is based on the full energy balance. When snow density on glaciers reaches the density of glaciers, the snow becomes a part of glaciers. The influence of wind on turbulent flux and snow density is also considered (Shrestha et al., 2010). From this point of view, the model can simulate both the advance and melt of glaciers. An observation-based rain-snow temperature threshold data set developed by Jennings et al. (2018) was used, which avoids uncertainty introduced by the calibration/subjective selection of the threshold. The overall structure of WEB-DHM-S can be found in Figure S1 in Supporting Information S1. The energy for melt (Q_M) is calculated as the sum of net shortwave radiation ($Q_{S\text{-Net}}$) and net longwave radiation ($Q_{L\text{-Net}}$) minus sensible heat flux (Q_H), latent heat flux (Q_L) and conductive heat flux (Q_G):

$$Q_M = Q_{S-\text{Net}} + Q_{L-\text{Net}} - Q_H - Q_L - Q_G \tag{1}$$

$$Q_H = \rho_{\text{air}} \cdot c_p \cdot C_d \cdot u \cdot (T_S - T_a) \tag{2}$$

$$Q_L = \rho_{\text{air}} \cdot L_v \cdot C_d \cdot u \cdot (q_S - q_a) \tag{3}$$

$$Q_{S-\text{Net}} = Q_{S-\text{downward}} \cdot (1 - \partial) \tag{4}$$

where Q_M is the energy for melt; $Q_{S-\text{Net}}$ and $Q_{L-\text{Net}}$ are net shortwave and longwave radiation, respectively; Q_H is sensible heat flux; Q_L is latent heat flux; Q_G is conductive heat flux; ρ_{air} is the density of air; C_p is the specific heat of air; L_v is the latent heat of vapourization; C_d is the bulk coefficient; u is the wind speed; T_S is the temperature of surface; T_a is the air temperature; q_S is the surface specific humidity; q_a is the specific humidity of air.; $Q_{S-\text{downward}}$ is the downward solar radiation; ∂ is the albedo and its parameter values used can be found in Table S1 in Supporting Information S1. Albedo variations are simulated using the Biosphere-Atmosphere Transfer Scheme model. In this study, the WEB-DHM-S model was run using a daily time step at a 0.1 degree spatial resolution. More detailed descriptions about the physical processes of WEB-DHM-S can be found in the studies by Sellers, Randall, et al. (1996), Sellers, Tucker, et al. (1996), Shrestha et al. (2010, 2015), and L. Wang et al. (2016).

The initial condition for the modeling was the soil moisture information. Our simulation was performed from the first day of every year to derive spatially variable soil moisture information. The initial condition of 2021 was assumed the same as the first day of 2011. Because we studied the multiyear mean glacier and snow melt contributions to discharge, the initial condition would have minor influence on the overall results. The observed discharge data in the historical period ended in 2010. The historical period simulation ended in 2011 to ensure the historical simulation was 30 yr (1982–2011). We started the future simulation in 2021, and ended the simulation in 2050 to keep the years of future simulation the same as the historical period. Because the mass balance is negative in the studied glaciers, we used the melt rate (m w.e./yr) to represent the mass balances (m w.e./yr). The normalized glacier area fraction is defined as $(f - f_{\text{min}})/(f_{\text{max}} - f_{\text{min}})$, where f is the glacier area fraction and f_{min}

Table 2
Model Parameters and Regional Average Rain-Snow Temperature Thresholds

Symbol (unit)	River basin						
	Yarlung Tsangpo River	Upper Nu River	Upper Lancang River	Upper Yangtze River	Yalong River	Min River	Upper Yellow River
KS (m/s)	1.98E-05	1.61E-06	9.44E-08	2.75E-06	5.75E-05	5.63E-07	1.63E-04
anik	0.29	1.86	2.93	0.65	0.12	10.21	2
Smax (m)	9.10E-04	1.05E-02	3.05E-02	8.38E-02	3.20E-02	1.27E-01	3.84E-01
Θs (m^3/m^3)	0.89	0.62	0.61	0.75	0.89	0.58	0.82
alpha	4.29E-02	1.87E-02	1.09E-02	1.11E-02	1.30E-02	7.94E-03	1.28E-02
n	2.73	2.25	1.41	1.55	1.71	3.41	1.62
f	2.16	3.83	5.11	4.73	3.56	4.93	0.86
Ts (K)	275.84	275.7	275.73	276.03	275.56	275.22	276.05

Note. "Ts" represents average values of rain-snow temperature thresholds in the river basins. KS: saturated hydraulic conductivity for soil surface; anik: hydraulic conductivity anisotropy ratio; Smax: Maximum ground surface water interception; Θs: Saturated water content; alpha: van Genuchten parameter (van Genuchten, 1980); *n*: van Genuchten parameter (van Genuchten, 1980); *f*: Hydraulic conductivity decay factor.

and f_{max} are the minimum and maximum glacier area fraction in the river basins, respectively (Brun et al., 2017; Miles et al., 2021).

2.4. Influence of Rain-Snow Temperature Threshold

There are two experiments when studying the influence of rain-snow temperature threshold. The first is the mean rain-snow temperature (Ts) scenario in which the spatial distribution of rain-snow temperature thresholds is not considered and the regional average of Ts is used to separate snowfall from precipitation. The second is the 273.15 K scenario which is traditionally used to separate snowfall from precipitation.

3. Results

3.1. Model Evaluation

Table 2 shows calibrated model parameters. Model performances in discharge simulation are shown in Table 3. The overall performances in the discharge simulation are satisfactory, with the Nash-Sutcliffe efficiency (NSE) and relative bias (RB) values reaching 0.96 and −1.3%, respectively. Figure 2 shows the observed and simulated discharge comparison in the rivers. The modeled discharge variations replicate the observations very well.

Table 3
Model Performance in Discharge Simulation

River basin	Hydrological gauge	Calibration		Validation		Overall	
		NSE	RB	NSE	RB	NSE	RB
Yarlung Tsangpo River	Nuxia (*1982–1996*, **1997–2010**, 1982–2010)	0.84	16.6%	0.97	−1.5%	0.94	6.8%
Upper Nu River	Jiayuqiao (*1982–1992*, **1993–2000**, 1982–2000)	0.95	4.4%	0.93	−9.6%	0.95	−3.7%
Upper Lancang River	Changdu (*1982–1996*, **1997–2010**, 1982–2010)	0.88	−3.8%	0.9	−1.1%	0.90	−2.5%
Upper Yangtze River	Shigu (*1982–1991*, **1992–2000**, 1982–2000)	0.92	−6.0%	0.95	−1.9%	0.94	−4.1%
Yalong River	Ertan (*1982–1993*, **1994–2005**, 1982–2005)	0.89	−1.1%	0.85	−1.6%	0.87	−1.3%
Min River	Wutongqiao (*1982–1991*, **1992–2002**, 1982–2002)	0.95	−2.8%	0.96	−2.2%	0.96	−2.5%
Upper Yellow River	Tangnaihai (*1982–1996*, **1997–2010**, 1982–2010)	0.81	4.3%	0.85	3.0%	0.84	3.7%

Note. The time periods in the brackets represent calibration (italic type), validation (bold type) and overall periods, respectively.

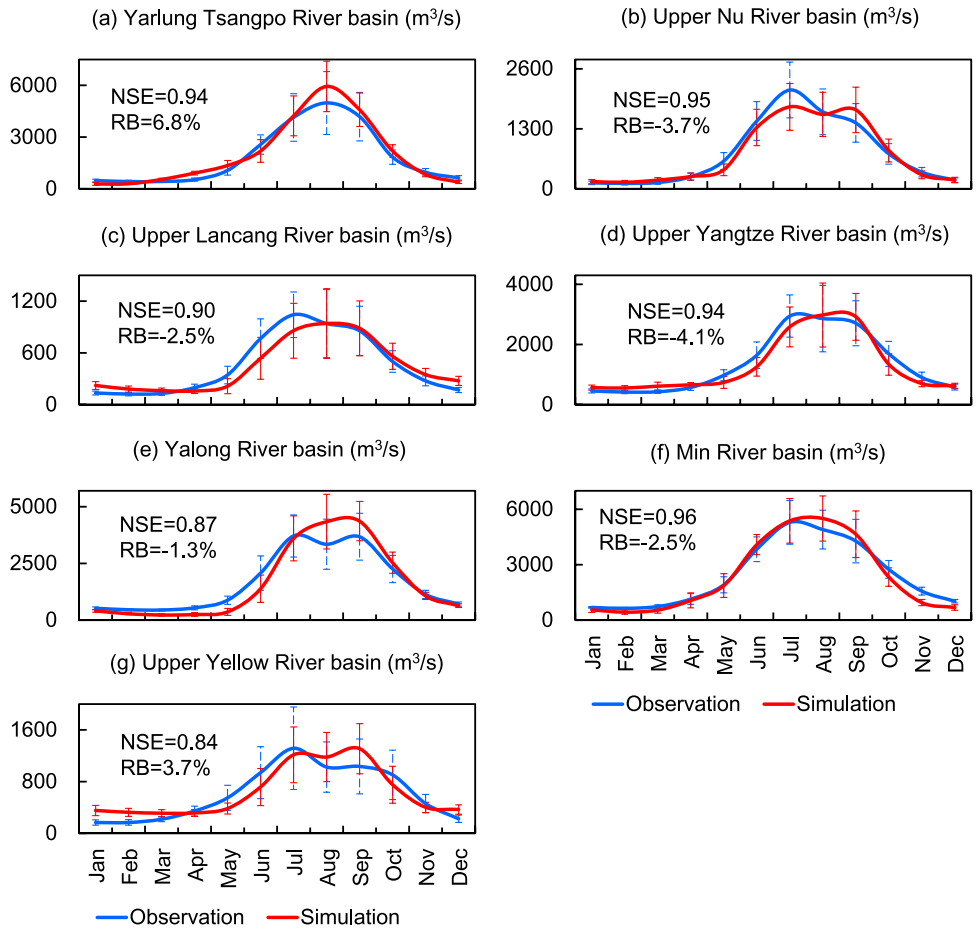

Figure 2. Observed and simulated discharge comparisons on a multiyear mean monthly scale in the river basins studied. The bars represent the standard deviation based on interannual average for the given month.

Figure 3 shows MODIS-observed and simulated snow cover fraction comparisons. The model simulates the variations of snow cover fractions very well, with R and |RB| (absolute value of RB) values reaching 0.97 and 2.4%, respectively. Because the GRACE data have a coarse spatial resolution of 3 × 3 degrees, we evaluated our simulated TWSCs in the entire study region based on the GRACE data. Figure 4 shows the comparison of TWSCs. The GRACE data do not have data for several months before August 2003 and after November 2010. The comparison of TWSCs was based on data from August 2003 to November 2010. The simulated and GRACE observed slope values of TWSCs are 0.03 mm/month and 0.02 mm/month, and the correlation coefficient value of the TWSC comparison reaches 0.7, indicating acceptable model performance.

3.2. Glacier Melt Rate

Glacier melt rates varied greatly among river basins, and all the river basins showed that the glacier melt was accelerating. The eastern part of the Yarlung Tsangpo River basin (the lower reach) had the highest glacier melt rates (Figure 5a). The average glacier melt rate in the Yarlung Tsangpo River Basin was also the greatest among all the river basins (0.40 ± 0.01 m w.e./yr, Figure 5b). In the Yarlung Tsangpo River, the energy input from downward shortwave and longwave radiation was the highest among all the river basins (Table 4), the snowfall was the lowest among the rivers, and the temperature was relatively higher than others except for the Yalong River. The combined effects of the radiation, snowfall, and air temperature could lead to the relatively larger glacier melt rate in the Yarlung Tsangpo River. The average glacier melt rate in the entire region was 0.32 ± 0.007 m w.e./yr, and the mean trend was 0.42 mm/yr (Figure 6a).

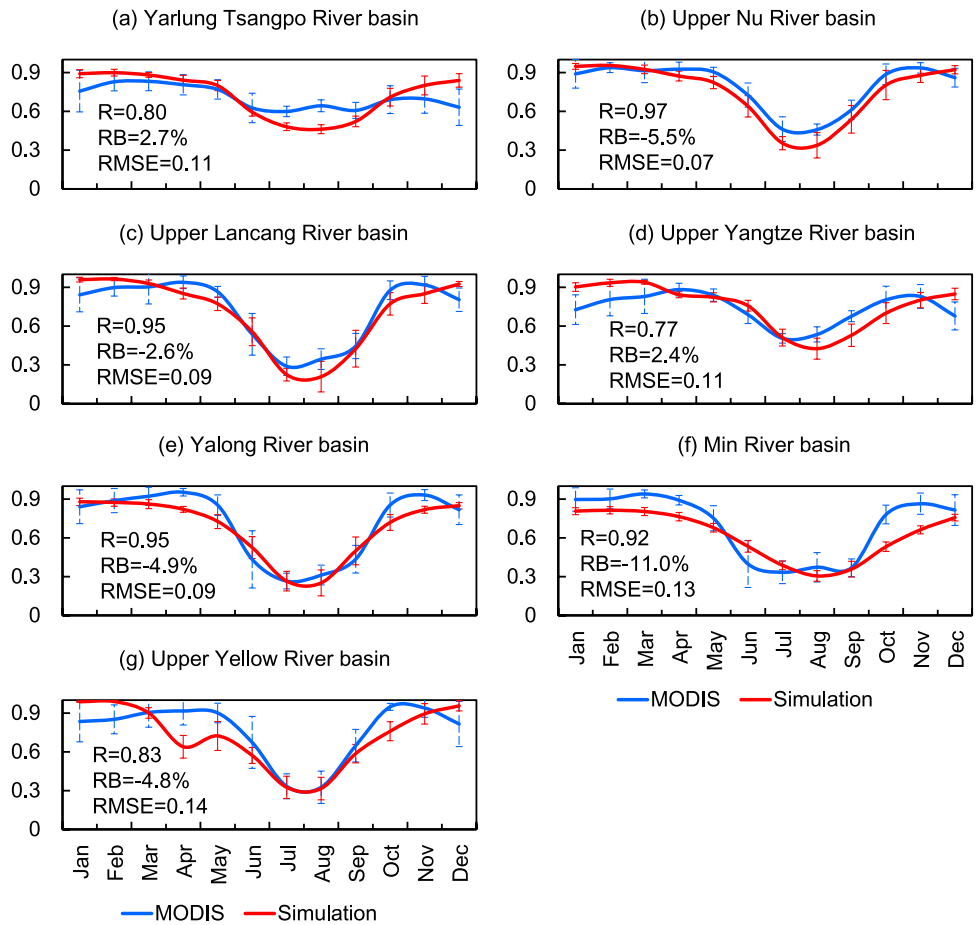

Figure 3. MODIS observed and simulated snow cover fraction (snow-covered area/total area) comparisons on a multiyear mean monthly scale. The bars represent the standard deviation based on interannual average for the given month.

The trend of glacier melt was consistent with air temperature, downward longwave radiation and humidity but different from the trends of downward shortwave radiation and wind speed (Figure 6). Although the precipitation was increasing (Figure 6h), the snowfall was decreasing (Figure 6g) because of the increasing air temperature. The reducing snowfall could result in decreases of the glacier accumulation. Q_H could decrease (Figure 7b) with increasing air temperature which could result in increases in the energy for melt. Therefore, warming climate could lead to increases in glacier melt. The increasing specific humidity of air (Figure 6f) could decrease Q_L

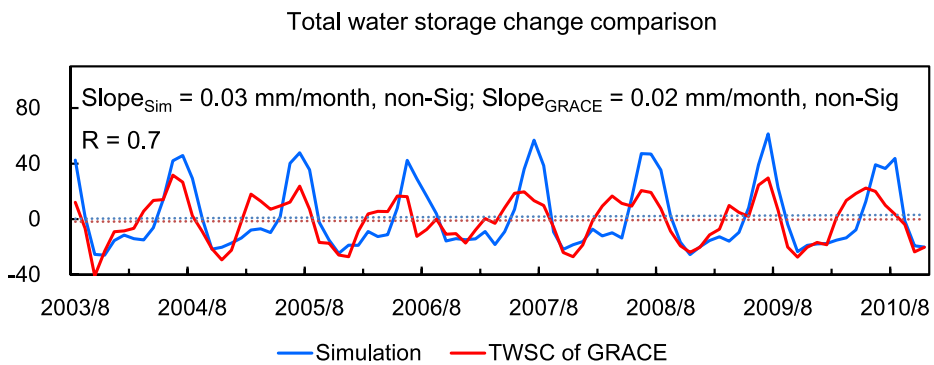

Figure 4. Total water storage change comparison between the model simulation and GRACE data from August 2003 to November 2010. Sig, significant. R, correlation coefficient.

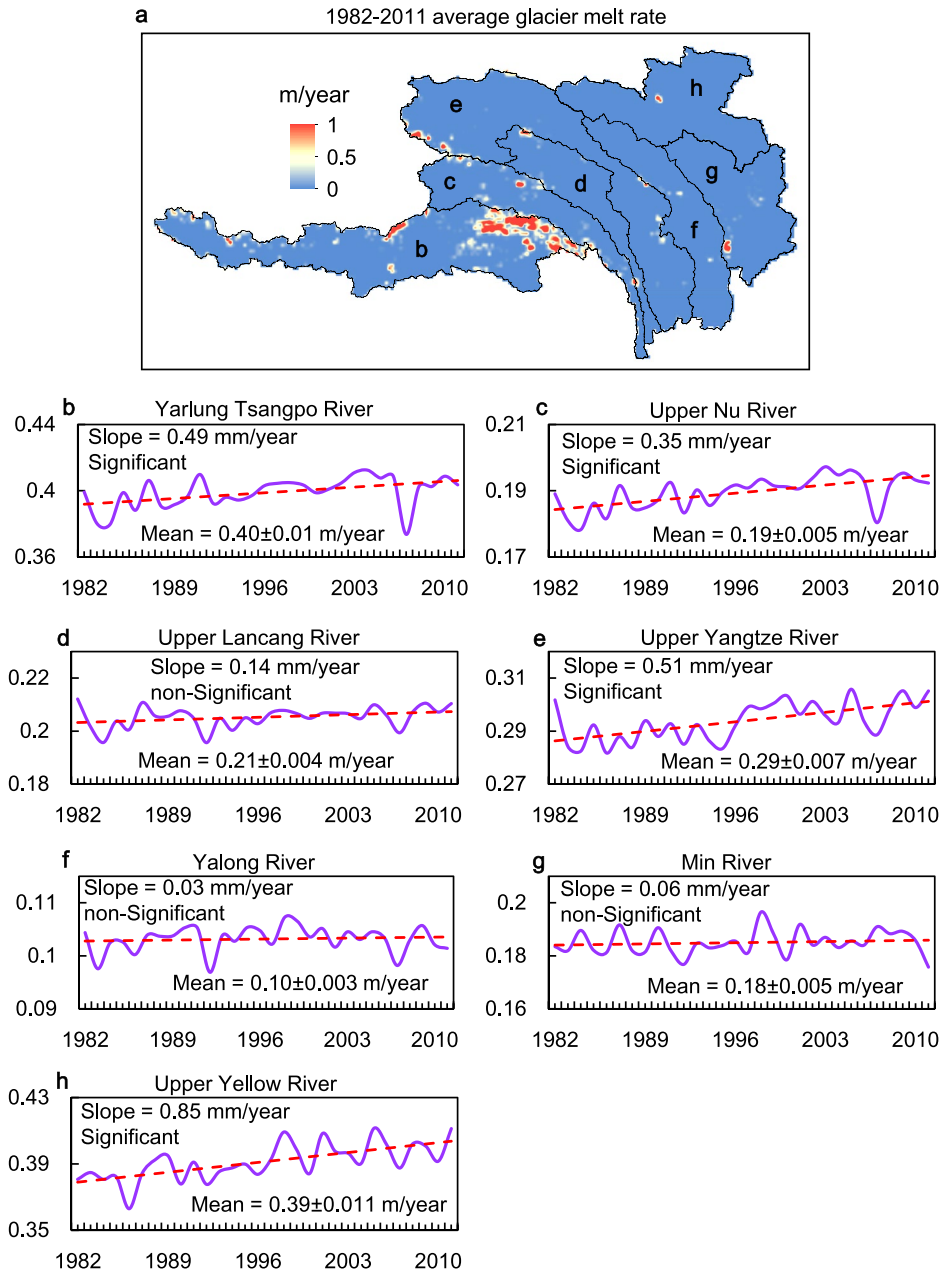

Figure 5. Spatial distribution of the glacier melt rate and river basin average glacier melt rate. The error values represent the standard deviation.

(Figure 7c) and therefore increase the energy for melt. When wind speed decreases (Figure 6e), Q_H and Q_L could decrease (Figures 7b and 7c), and the resulted energy for melt could increase which leads to growth in the glacier melt rate. The increasing downward longwave radiation (Figure 6c) could result in the increase in the net radiation, which could increase the energy for melt. Therefore, the increasing glacier melt energy (Figure 7e) was the combined results of the increasing air temperature, specific humidity, and downward longwave radiation and the decreasing wind speed. The increasing glacier melt energy could result in the increasing glacier melt rate.

In 2007, the snowfall was relatively low (Figure 7g) implying that the glacier accumulation because of snowfall supply was not much. Compared to the previous year 2006, the downward shortwave radiation reduced 7.3 w/m^2, and downward longwave radiation increased 2.2 w/m^2 in 2007. The net shortwave radiation reduced 4.4 w/m^2 in 2007 compared to 2006. The reduced net shortwave radiation doubled the increase in the downward

Table 4
Mean and Slope of Linear Trends of Meteorological Variables in Glacier Covered Area During 1982–2011

River basin	*T* (K)	Rs (w/m^2)	Rl (w/m^2)	Rs + Rl (w/m^2)	Precipitation (*snowfall*) (mm/month)
Yarlung Tsangpo River	270.5 (0.08, Sig)	214.8 (−0.19, Sig)	234.5 (0.37, Sig)	449.3	49.7(23.8) (0.09, non-Sig, −0.24, Sig)
Upper Nu River	269.8 (0.08, Sig)	206.5 (0.16, Sig)	233.9 (0.24, Sig)	440.4	55.7(29.2) (0.16, non-Sig, −0.18, Sig)
Upper Lancang River	268.7 (0.05, Sig)	208.5 (−0.26, non-Sig)	228.2 (0.30, Sig)	436.7	54.7(28.4) (0.11, non-Sig, −0.16, Sig)
Upper Yangtze River	268.0 (0.06, Sig)	215.1 (−0.20, Sig)	223.7 (0.28, Sig)	438.8	48.4(26.6) (0.19, Sig, −0.06, non-Sig)
Yalong River	271.6 (0.04, Sig)	195.6 (−0.41, Sig)	244.4 (0.31, Sig)	440.0	76.8(31.1) (−0.22, non-Sig, −0.27, Sig)
Min River	270.3 (0.06, Sig)	169.7 (−0.06, non-Sig)	247.6 (0.25, Sig)	417.3	100.4(55.7) (−0.47, Sig, −0.59, Sig)
Upper Yellow River	266.5 (0.05, Sig)	206.7 (0.07, non-Sig)	219.0 (0.13, Sig)	425.7	37.3(31.2) (0.03, non-Sig, −0.11, non-Sig)

Note. Data in the brackets represent slope and significance. *T*, air temperature; Rs, downward shortwave radiation; Rl, downward longwave radiation; "Sig", significant. The significance was evaluated at a 0.05 level based on the nonparametric Mann-Kendall analysis approach. The italic type in the last column shows the snowfall and its trends.

longwave radiation. The reduced downward shortwave radiation and other energy components resulted in that the net radiation in 2007 (106.68 w/m^2) was lower than 2006 (108.78 w/m^2; Figure 7a). In 2007 and 2008, the net radiation was 106.68 and 102.98 w/m^2, and the ground heat flux was 84.85 and 78.98 w/m^2, respectively. In 2007, the larger downward shortwave radiation in April and May (the cold season) could lead to higher penetrating shortwave radiation, and therefore could increase the ground heat flux (Zhu et al., 2018). When subtracting the ground heat flux from the net radiation, the larger ground heat flux could lead to relatively lower glacier melt energy in 2007 than in 2008. Overall, the downward shortwave radiation may lead to the relatively lower glacier melt energy in 2007 (3.21 w/m^2) than other years as shown in Figure 7e (e.g., 3.45 w/m^2 in 2006 and 3.42 w/m^2 in 2008), and therefore the lower glacier melt rate in 2007.

3.3. Historical Snow and Glacier Melt Contributions to Discharge

Glacier and snow melt contributions to discharge differed substantially among the river basins, and the average contribution from snow melt was larger than that from glacier melt. Glacier melt contributions were greater in the Yarlung Tsangpo, Upper Nu, and Upper Yangtze River Basins than that in the other basins (Figure 8a). The highest and lowest glacier melt contributions were from the Yarlung Tsangpo River Basin (19.8%) and the Yalong River Basin (0.6%), respectively, which was because the Yarlung Tsangpo River Basin and the Yalong River Basin had the largest and smallest glacier areas, respectively (Table 1, Figure 8c). The mean glacier melt contribution to discharge was 7.6% in the studied river basins. Snow melt contributions were higher in the Upper Yangtze and Upper Lancang River Basins (≥14%) than that in the other basins, and were the lowest in the Upper Yellow River Basin (5.6%). The average snow melt contribution to discharge in the region was 10.0%.

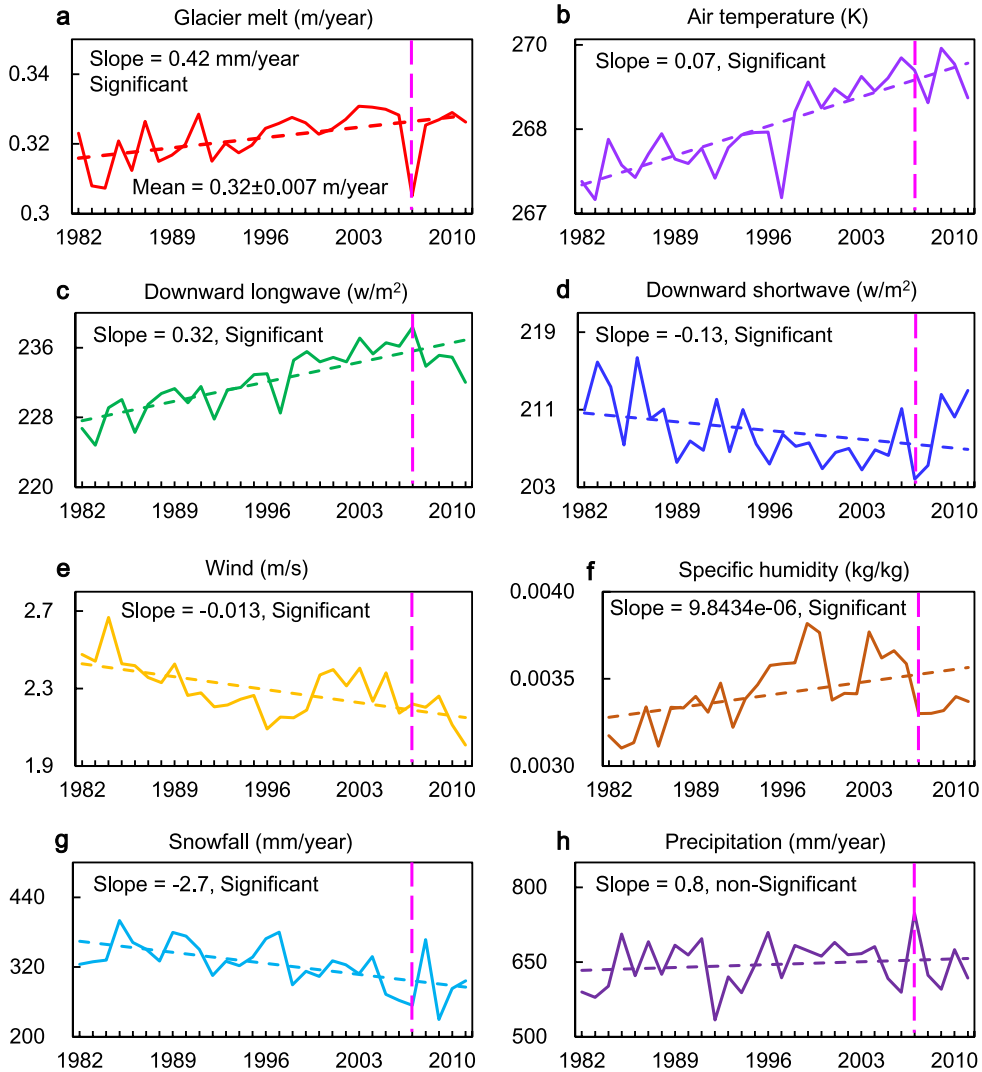

Figure 6. Temporal changes in the regional average glacier melt rate and climate from 1982 to 2011. The pink vertical lines indicate the values in 2007. The error in the mean glacier melt rate represents the standard deviation.

Contributions from snow and glacier melt to total discharge diverged spatially (1982–2011), and the closer to the glaciers, the larger the glacier melt contribution to discharge. The lower reaches of the Yarlung Tsangpo River and Upper Yangtze River Basins had relatively larger snow melt discharges than other river basins (Figure S2a in Supporting Information S1). Relatively higher glacier melt discharge was found in the lower reach of the Yarlung Tsangpo River Basin (Figure S2b in Supporting Information S1), which was due to the large glacier volume. For total discharge, the lower reaches of the Yarlung Tsangpo, Upper Yangtze, Yalong, and Min Rivers had relatively larger discharges than other regions (Figure S2c in Supporting Information S1). Regarding snow melt contribution to total discharge, the Upper Yellow and Yalong River Basins had smaller contributions than others (Figure 9a). For the glacier melt contribution, regions near the glaciers showed higher glacier melt contribution percentage (Figure 9c). This was especially true in the lower reach of the Yarlung Tsangpo River Basin, which had a large glacier volume.

3.4. Future Snow and Glacier Melt Contributions to Discharge

Future snow and glacier melt contributions to discharge would change differently in space under the RCP8.5 extreme climate scenario (Figures 9b, 9d, and 10). Generally, the larger the glacier cover fractions in the basins,

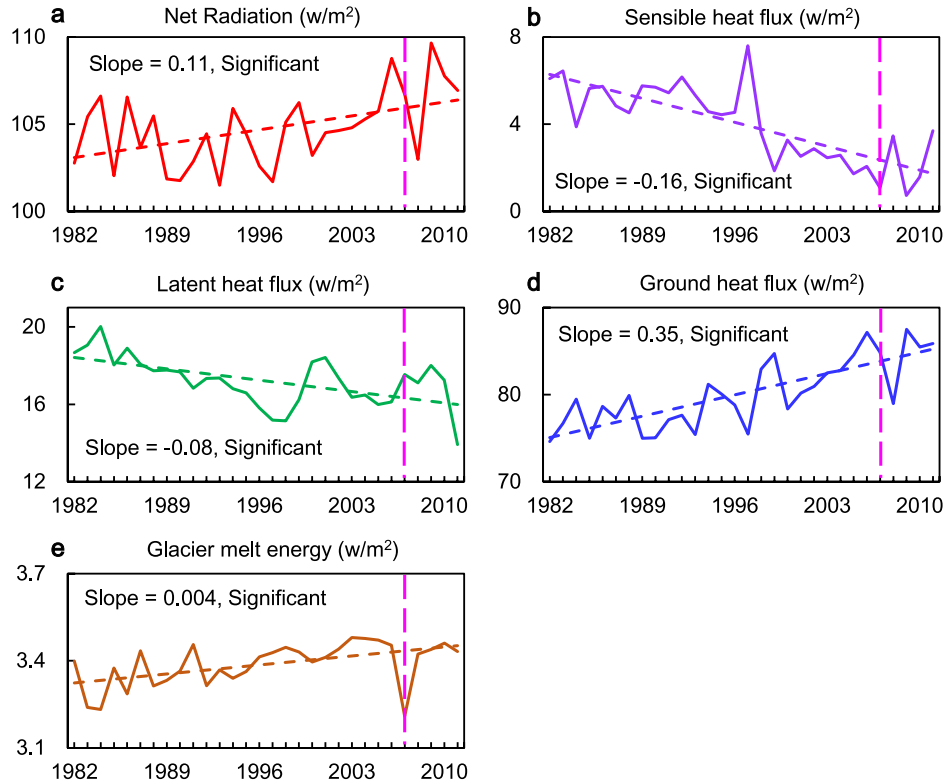

Figure 7. Temporal changes in the regional average energy components. The pink vertical lines indicate the values in 2007.

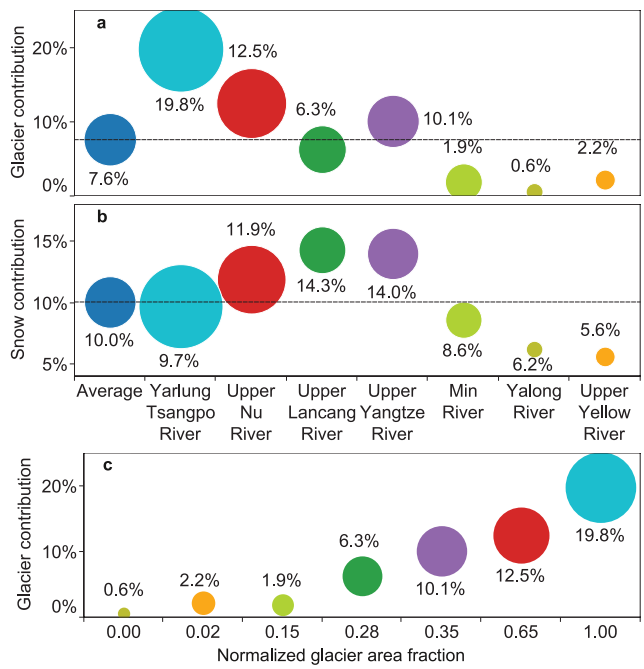

Figure 8. Historical relative contributions of glacier and snow melt to discharge in the hydrological gauges in Figure 1 (a, b), and variations of the glacier contributions with normalized glacier area fraction in each basin (c). In (a and b), the larger the circles, the greater the glacier cover fraction in the river basins; in (c), the larger the circles, the greater the glacier melt contributions. The dashed lines represent the average values.

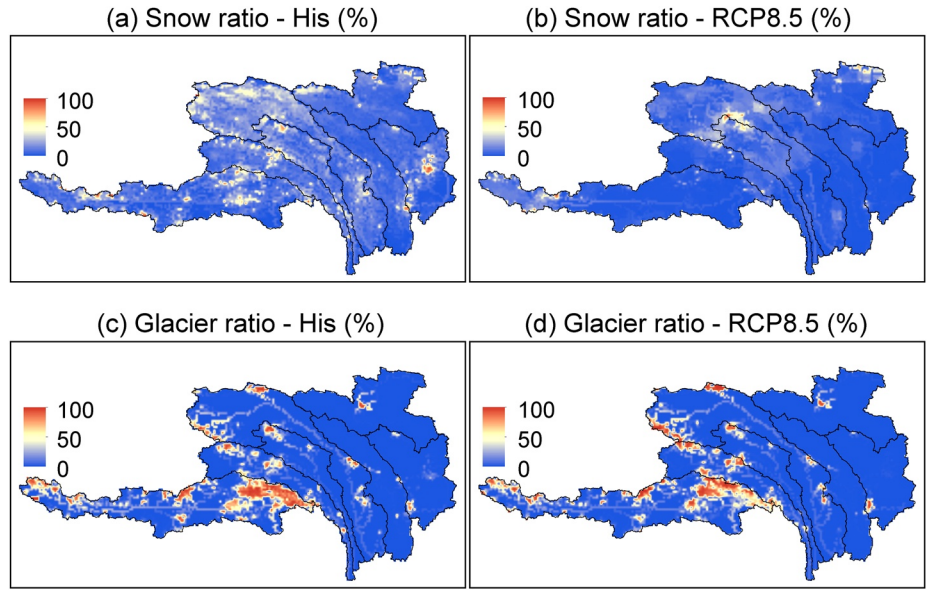

Figure 9. Multiyear mean spatial distribution of snow and glacier ratios in the baseline period (His, 1982–2011) and future period (RCP8.5, 2021–2050). His, baseline period. Ratio, snow or glacier melt discharge/total discharge × 100.

the greater the glacier melt contributions to discharge (Figure 10c). The Upper Lancang River Basin would have the largest snow melt contribution to discharge: 10.7% [7.7%, 13.0%] (Table 5), and the Min River Basin would have the smallest contribution: 1.1% [0.9%, 1.4%] (Table 5). The glacier melt contribution to discharger would be the largest in the Yarlung Tsangpo River Basin (18.4% [13.1%, 21.2%]), and the least in the Yalong River (0.7% [0.5%, 0.8%]). The relative contribution of snow melt to discharge would decrease in all the river basins, and the average relative contribution of snow melt would decrease to 4.5%. The greatest change in the relative contribution of snow melt would occur in the Upper Nu River Basin (−8.8%), and the smallest change would occur in the Upper Yellow River Basin (−1.8%). In contrast, the relative contribution of glacier melt would have a relatively minor overall change (−0.2%), and the largest decrease in the relative contribution of glacier melt would occur in the Yarlung Tsangpo River Basin (−1.4%). The sum of the relative contributions of snow and glacier melt would decrease in all the river basins, and the average of the changes would be −5.7%. Among all the river basins, the sum in the Upper Nu River Basin would decrease the most (−9.2%), and the sum in the Upper Yellow River would decrease the least (−2.2%). In the Upper Nu River, the relatively larger decrease in the total contributions of snow and glacier melt runoff would be the combined results of the relative changes in total, snow melt, and glacier melt runoff. The snow runoff in the Upper Nu River would reduce by 71.2% compared to the baseline period, which is less than the reductions in the Min (87.1%) and Yalong (80.5%) Rivers. The total runoff would increase by 10.9% in the Upper Nu River, but would reduce by 2.7% in the Yalong River and increase by 5.2% in the Min River. In addition, the increase of glacier melt runoff would be lower in the Upper Nu River (6.9%) than that in the Min River (28.0%). The combined effects would also result in the least reduction of the sum of snow and glacier melt contributions in the Upper Yellow River. The snow runoff would reduce by 13.4% (the lowest among the rivers), and the total runoff would increase by 28.9% (the highest among the rivers) in the Upper Yellow River.

Absolute values of glacier melt runoff would increase in most of river basins, with the exceptions in the Yalong and Upper Lancang River Basins (Table 6). The increases in glacier melt runoff would be the largest in the Min River Basin (28.0%) and Yarlung Tsangpo River Basin (12.2%). In the Min River Basin, both the air temperature and downward shortwave radiation would increase during the 2021–2050 period, which would likely result in the largest relative increase in glacier melt runoff. In the Yarlung Tsangpo River Basin, glacier melt runoff would be the greatest among all the river basins during the 2021–2050 period. Although glacier melt runoff would decrease in the Yalong and Upper Lancang River Basins, the decrease would be minor (only 0.2 m^3/s). Absolute values of snow runoff would decrease in all the rivers, which would be because the warming trends would decrease snowfall. Air temperature in the Min River Basin would increase the most (4.6°C), and air temperature would increase

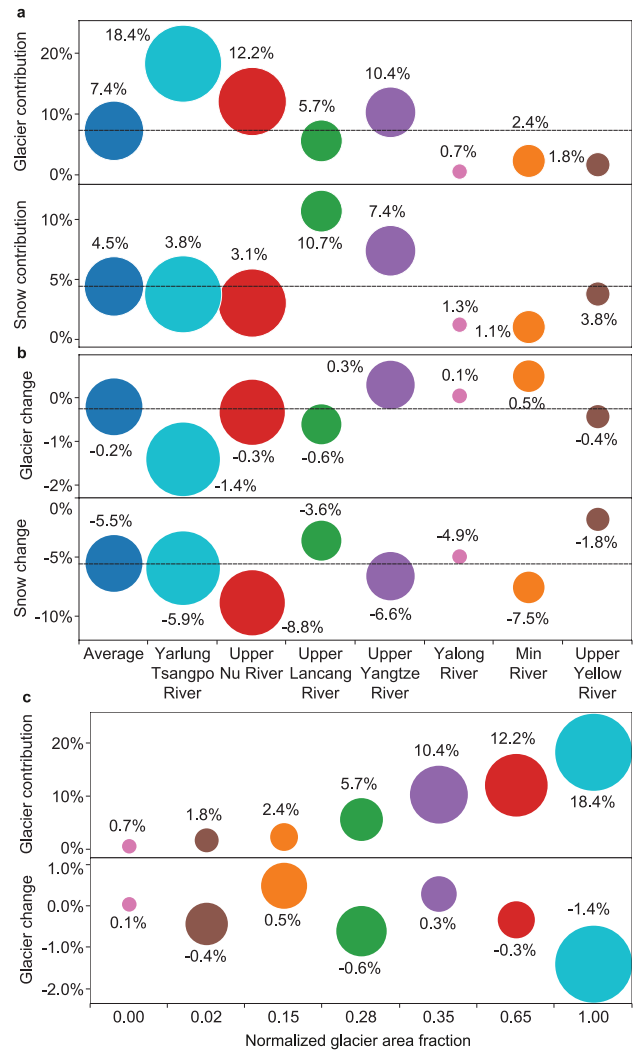

Figure 10. Relative contributions of glacier and snowmelt to discharge at the hydrological stations in Figure 1 during 2021–2050 under the RCP8.5 scenario (a), changes compared to 1982–2011 (b), and variations of the glacier contributions and changes with normalized glacier area fraction in each basin (c). Change = average of 2021–2050 minus average of 1982–2011. In (a and b), the larger the circles, the greater the glacier cover fraction; in (c), the larger the circles, the greater the glacier melt contributions or changes. The dashed lines represent the average values.

the least in the Upper Lancang River Basin (0.8°C). Correspondingly, the snowfall would decrease the most in the Min River (71.6%), and the least in the Upper Lancang River (20.5%).

The total runoff would increase in all the river basins with the exception of the Yalong River Basin where the decrease would be minor (only 2.7% as shown in Table 6). In the Yalong River, the decrease in total runoff would be the combined results of the decreasing precipitation, reducing glacier melt runoff and the increasing evapotranspiration. In the Upper Lancang River Basin, precipitation and evapotranspiration would decrease by 1.1% and 11.6%, respectively. The relatively more decrease in evapotranspiration than precipitation would lead to the increase in total runoff in the Upper Lancang River. Similarly, in the Upper Yangtze River, precipitation and evapotranspiration would decrease by 3.8% and 6.3%, respectively, which would lead to the increase in the total runoff in addition to the increase in the glacier melt runoff. In the Yarlung Tsangpo River, Upper Nu River, Min River, and Upper Yellow River, both precipitation and glacier melt runoff would increase, which would lead to the increases in the total runoff.

Table 5
Bounds of Relative Contributions of Snow and Glacier Melt to Total Runoff

River basin	2021–2050 ([min, max])	
	Snow	Glacier
Yarlung Tsangpo River	[3.1%, 5.1%]	[13.1%, 21.2%]
Upper Nu River	[2.4%, 3.8%]	[10.2%, 13.0%]
Upper Lancang River	[7.7%, 13.0%]	[4.8%, 6.2%]
Upper Yangtze River	[5.3%, 9.8%]	[9.4%, 11.2%]
Yalong River	[0.9%, 1.6%]	[0.5%, 0.8%]
Min River	[0.9%, 1.4%]	[2.3%, 2.5%]
Upper Yellow River	[3.0%, 4.9%]	[1.6%, 1.9%]

Note. The minimum (min) and maximum (max) values are based on the simulation ensemble using the GCMs under the RCP8.5.

3.5. Influence of Rain-Snow Temperature Threshold

The rain-snow temperature threshold influences the estimated snow melt contribution to discharge (Table 7). Similar to the results of considering the spatial distribution of Ts, the snow melt contributions are higher in the Upper Lancang and Upper Yangtze River Basins than that in other basins, and the contribution in the Upper Yellow River Basin is less than or equal to the contributions in other river basins. In the mean Ts scenario, the average contribution of snow melt to total discharge is 9.6%, which is close to the result (10.0%) when considering the spatial distribution of the rain-snow temperature thresholds, suggesting that the spatial heterogeneity of rain-snow temperature thresholds has a minor influence on the estimated snow melt contribution. In the 273.15 K scenario, the largest snow melt contribution is in the Upper Nu River Basin (4.0%), and the smallest snow melt contribution is in the Yalong River Basin (2.0%). Compared to the estimated snow melt contribution in the mean Ts scenario, the results in the 273.15 K scenario change markedly and show a smaller snow melt contribution. The estimated average contribution of snow melt is 3.2% in the 273.15 K scenario, which is three-fold (9.6%/3.2% = 3) lower than that in the mean Ts scenario, suggesting that the traditionally used 273.15 K rain-snow temperature threshold could lead to remarkable underestimations of snow melt contributions to total discharge. Overall, the rain-snow temperature threshold may have influenced the differences in the estimated snow and glacier melt contributions between our study and previous studies, since previous studies used the 273.15 K or regional average rain-snow temperature threshold values.

3.6. Sensitivity Analysis

The sensitivity of glacier melt is analyzed by perturbing the climate variables (Table 8). When increasing the air temperature by 2.5%, the glacier melt rate would increase by 15.45%; when reducing the air temperature by 2.5%, the glacier melt rate would decrease by 9.46%. For other climate variables, increasing downward shortwave and longwave radiation and specific humidity would lead to increases in the glacier melt, and decreasing wind would increase the glacier melt. The relative changes in the glacier melt resulted from downward shortwave and longwave variations are comparable, and are lower than the change percentages because of air temperature variations. Compared to others, the resulted changes because of specific humidity and wind speed are minor. The results indicate that glacier melt is more sensitive to air temperature, downward shortwave, and longwave radiation than specific humidity and wind speed when their relative changes are the same. Although the 2.5% perturbation is selected subjectively, the results demonstrate that increasing (decreasing) air temperature, downward shortwave and longwave radiation and specific humidity can increase (decrease) glacier melt, and that decreasing (increasing) wind speed can increase (decrease) glacier melt in the whole of eastern and southern TP.

4. Discussion

4.1. Comparisons With Other Studies and Implications

In contrast to many previous studies, our study considers the full energy balance in the glacier and snow melt in the whole of eastern and southern TP. Therefore, the influence of downward shortwave and longwave radiation on glacier melt trend and melt rate fluctuation can be analyzed for the large-scale region in addition to the influence from other climate variables. Our study found that air temperature, downward longwave radiation, humidity, and wind speed determined the overall glacier melt trend, and downward shortwave radiation played an additional role in influencing the fluctuation of glacier melt rates. No similar findings have been reported before in the whole of eastern and southern TP. Previous modeling studies did not consider the downward shortwave and/or longwave radiation, humidity, and wind speed in the region, and therefore the influences were not studied. For example, Zhang et al. (2013, 2019) used the variable infiltration capacity model but combined with a degree-day glacier melt scheme; Lutz et al. (2014) used a cryospheric-hydrological model but also combined with the degree-day scheme; Chen et al. (2017) and Han et al. (2019) used the coupled routing and excess storage model combined with the degree-day approach.

Table 6
Comparisons Between Future and Historical Hydro-Climate in Terms of Precipitation, Snowfall, Air Temperature, Downward Shortwave Radiation, Downward Longwave Radiation, Evapotranspiration, Total Runoff, Snow Runoff and Glacier Runoff

River basin	2021–2050 (1982–2011)								
	P (mm/yr)	*S* (mm/yr)	*T* (K)	Rs (w/m^2)	Rl (w/m^2)	ET (mm/yr)	Total runoff (m^3/s)	Snow runoff (m^3/s)	Glacier runoff (m^3/s)
Yarlung Tsangpo River	↑554.0 (456.6)	↓84.1 (156.9)	↑275.2 (272.2)	↓224.9 (235.7)	↑247.2 (233.7)	↑179.8 (135.1)	↑2,433.2 (1,987.0)	↓92.8 (192.3)	↑441.1 (393.0)
Upper Nu River	↑659.2 (632.6)	↓119.9 (234.8)	↑273.3 (270.8)	↓203.3 (215.4)	↑245.7 (234.7)	↓230.0 (246.4)	↑845.8 (762.5)	↓26.2 (91.0)	↑101.8 (95.2)
Upper Lancang River	↓624.3 (631.2)	↓157.2 (197.9)	↑272.3 (271.5)	↓198.4 (209.4)	↑248.5 (239.1)	↓279.3 (316.0)	↑496.9 (445.9)	↓53.8 (63.7)	↓28.1 (28.3)
Upper Yangtze River	↓513.2 (533.4)	↓113.8 (187.4)	↑272.7 (270.5)	↓201.7 (213.9)	↑243.6 (233.6)	↓311.2 (332.0)	↑1,363.5 (1,347.5)	↓102.1 (188.6)	↑141.1 (136.0)
Yalong River	↓796.2 (798.9)	↓73.8 (170.2)	↑278.3 (275.1)	↓196.8 (201.2)	↑271.6 (258.4)	↑361.4 (336.5)	↓1,521.8 (1,564.3)	↓19.1 (97.8)	↓9.5 (9.7)
Min River	↑945.0 (912.3)	↓53.4 (188.3)	↑282.2 (277.6)	↑170.7 (167.5)	↑290.6 (283.8)	↑342.8 (291.1)	↑2,409.0 (2,289.7)	↓25.6 (198.0)	↑57.1 (44.6)
Upper Yellow River	↑566.8 (492.4)	↓149.5 (240.7)	↑274.0 (270.6)	↓191.8 (207.5)	↑251.3 (235.0)	↑321.9 (292.6)	↑820.8 (636.8)	↓31 (35.8)	↑14.5 (13.9)

Note. "↑" and "↓" mean increase and decrease in 2021–2050 compared to 1982–2011. Data in the brackets represent averages in 1982–2011. *P*, precipitation; *S*, snowfall; *T*, air temperature; Rs, Downward shortwave radiation; Rl, Downward longwave radiation; ET, evapotranspiration.

In contrast to many previous studies, our study investigates all the river basins originated from the eastern and southern TP, quantitatively reveals the spatial distribution of snow and glacier melt contribution to discharge, and quantitatively reports the entire region's acceleration rate of the glacier melt for the 1982–2011 period: 0.42 mm/yr. A number of previous studies were carried out in one or two hydrological gauges/river basins in the region. They cannot provide an overall picture of glacier and snow melt contributions to discharge in the entire eastern and southern TP, cannot provide the spatial distribution of snow and glacier melt contributions to discharge, and cannot quantify the acceleration rate of glacier melt (e.g., Chen et al., 2017; Han et al., 2019; Makokha et al., 2016; Zhang et al., 2019; Zhou et al., 2015). In contrast to many previous studies, we calibrate/validate our simulation using multiple data sets, such as discharge, snow cover fraction, and water storage changes. Many previous studies did not validate their simulation comprehensively (e.g., Bookhagen & Burbank, 2010; Lutz et al., 2014; Pritchard, 2019; Su et al., 2016; Zhang et al., 2013). Therefore, uncertainty in their results could be large.

Comparison of our results with previous studies in terms of glacier mass balances is shown in Table 9. Generally, our results are close to the previous studies. For example, in the Nyainqentanglha region, our estimation is -0.44 ± 0.01 m w.e./yr, which is close to the studies by Shean et al. (2020; -0.50 ± 0.15 m w.e./yr), Brun et al. (2017; -0.62 ± 0.23 m w.e./yr), and Miles et al. (2021; -0.49 ± 0.08 m w.e./yr) based upon satellite data combined with additional observations for velocity and emergence. The differences may be because their time periods used are later and shorter than ours: 2000–2016 for Brun et al. (2017) and Miles et al. (2021), and 2000–2018 for Shean et al. (2020). Because the glacier melt is speeding up, the later time periods they used can result in higher glacier change rates than our estimation. Biemans et al. (2019) found that the sum of snow and glacier melt contributions to discharge ranged from 30% to 40% in the lower reach of the Yarlung Tsangpo River, and did not separate snow and glacier contributions. Our estimation is 9.7% for the snow melt and 19.8% for the glacier melt. The total of snow and glacier contributions is 29.5%, which is close to the estimation by Biemans et al. (2019).

Our study focused on the long-term annual mean trends in the eastern and southern TP, whereas most of previous studies in individual glaciers focused on internal/seasonal glacier variations (S. Li et al., 2018; Mölg et al., 2012; Zhu et al., 2015), which may be because their glacier data were short and not suitable for long-term trends analysis. Our results are consistent with smaller-scale studies generally. The Parlung No. 94 Glacier located in the southeast TP was found to be vulnerable to changes in air temperature (W. Yang et al., 2013), and the glacier melt fluctuation simulation considering downward shortwave radiation was found to be more practical and applicable than only considering the air temperature on a daily scale (W. Yang et al., 2011). Similarly, Zhu et al. (2018) suggested that the air temperature has remarkable impacts on glacier melt in the Parlung No. 4 and Zhadang glaciers in the southern TP, and that longwave and shortwave radiation also influenced glacier melt in the two glaciers. Liu et al. (2021) found that air temperature and radiation have more influence than precipitation on the Parlung No. 94 and Hailuogou glaciers in the eastern and southern TP. Compared to the studies in the individual glaciers, we provided an overall picture of glacier melt variations in the whole of southern and eastern TP.

Both our large-scale results and previous studies in individual glaciers show the shortwave radiation could influence fluctuations of glacier melt rate in the region. If the degree-day approach is used, the melt rate fluctuations would be overlooked to some degree in the past and future glacier melt simulation, though the overall trends would be reasonable. The TP is dimming (i.e., decreasing solar radiation) (Lin et al., 2019; K. Yang et al., 2012; You et al., 2009), which is related to aerosol and/or water vapor variations (Lin et al., 2019; K. Yang et al., 2012). The dimming phenomenon would continue in the future (as shown in Table 5 with the exception of the Min River). This phenomenon would influence glacier

Table 7
Snow Contribution to Discharge (1982–2011) Using Different Rain-Snow Temperature Thresholds

River basin	Hydrological gauge	Mean Ts	273.15 K
Yarlung Tsangpo River	Nuxia	9.6%	2.4%
Upper Nu River	Jiayuqiao	11.1%	4.0%
Upper Lancang River	Changdu	13.1%	3.8%
Upper Yangtze River	Shigu	14.2%	3.4%
Yalong River	Ertan	5.8%	2.0%
Min River	Wutongqiao	7.8%	4.0%
Upper Yellow River	Tangnaihai	5.8%	2.6%
Average		9.6%	3.2%

Note. Mean Ts values are shown in Table 2.

melt projections especially the melt rate fluctuations, and the impacts cannot be neglected because the future solar radiation reduction would be large (up to 7.6%). Therefore, energy balance-based approaches would be superior to the degree-day approach in glacier melt fluctuation projections in the southern and eastern TP in the future.

4.2. Limitations

We did not consider the influence of cloud directly. Because cloud can influence downward shortwave and longwave radiation, the impacts of cloud were considered through downward shortwave and longwave radiation implicitly in this study. Other snow falling on glaciers, such as snowfall variations caused by avalanche and wind, was not considered since these data are almost non-existent anywhere in the region.

Debris could reduce the energy reaching the glaciers. The thickness of the debris could influence the thermal resistance of the debris layer, and was not explicitly considered in the model because there was no accurate thickness information, which can be considered as a limitation of our study. In this study, the debris was considered as a single layer, and the thermal resistance of the debris layer was set to be 0.042 m^2/KW following the study by Shrestha et al. (2015) in a nearby region in the western TP. The albedo parameter values (Table S1 in the Supporting Information S1) and albedo variation simulation (based on the BATS model) followed the study by Shrestha et al. (2015). The study by Shrestha et al. (2015) showed that the model performed well in discharge simulation with considerations of glacier and snow melt: NSE of discharge simulation is 0.93, and average accuracy and absolute bias of areal extent of snow cover are 84% and 7%, respectively. Our study also shows the discharge and snow cover are simulated well and the average glacier melt rates are compatible with previous studies. Therefore, our methodology is appropriate. Although the lack of detailed debris thickness and the relatively coarse resolution may influence the results, the impacts could be minor because the debris-covered glacier area fraction is low (0.4%).

We used the rain-snow temperature threshold developed by Jennings et al. (2018) for the future periods, and did not consider the rain-snow threshold variations with climate change, which can be considered as a limitation of this study. Previous studies also used the threshold value in historical periods for future analysis, such as Berghuijs et al. (2014) and Kraaijenbrink et al. (2021). Although studies have investigated spatial variations of the rain-snow temperature threshold in historical periods (Ding et al., 2014), how future climate change would influence the thresholds is unknown at the moment. Future research is encouraged to investigate climate change influence on the rain-snow temperature threshold and resulting variations in snowfall and snow melt.

5. Conclusions

In this study, we adopted a physically based energy budget approach to study glacier and snow melt variations and their contributions to discharge in seven large river basins in the eastern and southern TP. Future projections were also carried out for a near-future time period under the RCP8.5 extreme climate scenario. The following main conclusions are presented on the basis of this study.

Table 8
Sensitivity of Glacier Melt to Changes in Climate Variables

	Change percentage	
Variable (perturbation)	+2.50%	−2.50%
Air temperature (±2.5%)	+15.45%	−9.46%
Downward shortwave radiation (±2.5%)	+1.10%	−1.08%
Downward longwave radiation (±2.5%)	+1.23%	−1.20%
Specific humidity (±2.5%)	+0.20%	−0.17%
Wind speed (±2.5%)	−0.12%	+0.16%

First, glacier was melting at a rate of 0.32 ± 0.007 m water equivalent/yr on average during 1982–2011 with large spatial variability, and it accelerated with a rate of 0.42 mm/yr.

Second, glacier and snow melt contributed 17.6% of annual river discharge on average during 1982–2011, and the contribution varied largely in space; it would likely decrease to 11.9% during 2021–2050 under the RCP8.5 scenario, due to decreases in snowmelt that are not offset by glacier melt increases.

Table 9
Comparison of Our Results With Previous Studies in Terms of Glacier Mass Balances (m w.e./yr)

Region	Study	Result
Yarlung Tsangpo River (Upper Brahmaputra River)	This study	-0.40 ± 0.01
Brahmaputra River	Brun et al. (2017)	-0.54 ± 0.22
Brahmaputra River	Pritchard (2019)	-0.50 ± 0.22
Yangtze River	This study	-0.29 ± 0.007
	Brun et al. (2017)	-0.35 ± 0.21
Nyainqentanglha Region	This study	-0.44 ± 0.01
	Miles et al. (2021)	-0.49 ± 0.08
	Shean et al. (2020)	-0.50 ± 0.15
	Brun et al. (2017)	-0.62 ± 0.23

Note. Upper Brahmaputra River includes ~60% of the glaciers in the Brahmaputra River.

Third, air temperature, downward longwave radiation, humidity, and wind speed determined the overall glacier melt trend, and downward shortwave radiation played an additional role in influencing the fluctuation of glacier melt rates.

Conflict of Interest

The authors declare no conflicts of interest relevant to this study.

Data Availability Statement

CMFD data were available in http://data.tpdc.ac.cn/en/data/8028b944-daaa-4511-8769-965612652c49/. CGDPA data were available in http://data.cma.cn/en. GRACE data were available in https://grace.jpl.nasa.gov/data/get-data/jpl_global_mascons/. ISIMIP2b data were available in https://www.isimip.org/gettingstarted/input-data-bias-correction/. Glacier data were available in https://www.glims.org/RGI/rgi60_dl.html.

Acknowledgments
This study was supported by the National Natural Science Foundation of China (92047202, 51809136, 41971304, and 41890852), Strategic Priority Research Program of the Chinese Academy of Sciences (XDA20060402), Shenzhen Science and Technology Innovation Committee (JCYJ20190809155205559), and Colleges Pearl River Scholar Funded Scheme 2018. Additional support was provided by Guangdong Provincial Key Laboratory of Soil and Groundwater Pollution Control (2017B030301012) and State Environmental Protection Key Laboratory of Integrated Surface Water-Groundwater Pollution Control. Wei Qi developed the concept and methodology for this study. Wei Qi performed the data analysis with support from Lian Feng, Xingxing Kuang, Chunmiao Zheng, Junguo Liu, Deliang Chen, Yong Tian, and Yingying Yao. All authors discussed the results and contributed to the preparation of the manuscript.

References

Azam, M. F., Kargel, J. S., Shea, J. M., Nepal, S., Haritashya, U. K., Srivastava, S., et al. (2021). Glaciohydrology of the Himalaya-Karakoram. *Science*, *373*(6557), eabf3668. https://doi.org/10.1126/science.abf3668

Azam, M. F., Wagnon, P., Vincent, C., Ramanathan, A. L., Favier, V., Mandal, A., & Pottakkal, J. G. (2014). Processes governing the mass balance of Chhota Shigri Glacier (western Himalaya, India) assessed by point-scale surface energy balance measurements. *The Cryosphere*, *8*(6), 2195–2217. https://doi.org/10.5194/tc-8-2195-2014

Berghuijs, W. R., Woods, R. A., & Hrachowitz, M. (2014). A precipitation shift from snow towards rain leads to a decrease in streamflow. *Nature Climate Change*, *4*(7), 583–586. https://doi.org/10.1038/nclimate2246

Biemans, H., Siderius, C., Lutz, A. F., Nepal, S., Ahmad, B., Hassan, T., et al. (2019). Importance of snow and glacier meltwater for agriculture on the Indo-Gangetic Plain. *Nature Sustainability*, *2*(7), 594–601. https://doi.org/10.1038/s41893-019-0305-3

Bolch, T., Kulkarni, A., Kääb, A., Huggel, C., Paul, F., Cogley, J. G., et al. (2012). The state and fate of Himalayan glaciers. *Science*, *336*(6079), 310–314. https://doi.org/10.1126/science.1215828

Bookhagen, B., Burbank, D. W. (2010). Toward a complete Himalayan hydrological budget: Spatiotemporal distribution of snowmelt and rainfall and their impact on river discharge. *Journal of Geophysical Research: Earth Surface*, *115*(F3). https://doi.org/10.1029/2009JF001426

Brun, F., Berthier, E., Wagnon, P., Kääb, A., & Treichler, D. (2017). A spatially resolved estimate of High Mountain Asia glacier mass balances, 2000–2016. *Nature Geoscience*, *10*(9), 668–673. https://doi.org/10.1038/ngeo2999

Chen, X., Long, D., Hong, Y., Zeng, C., & Yan, D. (2017). Improved modeling of snow and glacier melting by a progressive two-stage calibration strategy with GRACE and multisource data: How snow and glacier meltwater contributes to the runoff of the Upper Brahmaputra River basin? *Water Resources Research*, *53*(3), 2431–2466. https://doi.org/10.1002/2016WR019656

Datt, P., Srivastava, P. K., Negi, P. S., & Satyawali, P. K. (2008). Surface energy balance of seasonal snow cover for snow-melt estimation in N-W Himalaya. *Journal of Earth System Science*, *117*, 567–573. https://doi.org/10.1007/s12040-008-0053-7

Ding, B., Yang, K., Qin, J., Wang, L., Chen, Y., & He, X. (2014). The dependence of precipitation types on surface elevation and meteorological conditions and its parameterization. *Journal of Hydrology*, *513*, 154–163. https://doi.org/10.1016/j.jhydrol.2014.03.038

Farinotti, D., Huss, M., Fürst, J. J., Landmann, J., Machguth, H., Maussion, F., & Pandit, A. (2019). A consensus estimate for the ice thickness distribution of all glaciers on Earth. *Nature Geoscience*, *12*(3), 168–173. https://doi.org/10.1038/s41561-019-0300-3

Frieler, K., Lange, S., Piontek, F., Reyer, C. P. O., Schewe, J., Warszawski, L., et al. (2017). Assessing the impacts of 1.5°C global warming—Simulation protocol of the Inter-Sectoral Impact Model Intercomparison Project (ISIMIP2b). *Geoscientific Model Development*, *10*, 4321–4345. https://doi.org/10.5194/gmd-10-4321-2017

Gernaat, D., deBoer, H., Daioglou, V., Yalew, S. G., Müller, C., & van Vuuren, D. P. (2021). Climate change impacts on renewable energy supply. *Nature Climate Change*, *11*, 119–125. https://doi.org/10.1038/s41558-020-00949-9

Gudmundsson, L., Boulange, J., Do, H. X., Gosling, S. N., Grillakis, M. G., Koutroulis, A. G., et al. (2021). Globally observed trends in mean and extreme river flow attributed to climate change. *Science*, *371*(6534), 1159–1162. https://doi.org/10.1126/science.aba3996

Han, P., Long, D., Han, Z., Du, M., Dai, L., & Hao, X. (2019). Improved understanding of snowmelt runoff from the headwaters of China's Yangtze River using remotely sensed snow products and hydrological modeling. *Remote Sensing of Environment*, *224*, 44–59. https://doi.org/10.1016/j.rse.2019.01.041

He, J., Yang, K., Tang, W., Lu, H., Qin, J., Chen, Y., & Li, X. (2020). The first high-resolution meteorological forcing data set for land process studies over China. *Scientific Data*, *7*, 25. https://doi.org/10.1038/s41597-020-0369-y

Herreid, S., & Pellicciotti, F. (2020). The state of rock debris covering Earth's glaciers. *Nature Geoscience*, *31*(9), 621–627. https://doi.org/10.1038/s41561-020-0615-0

Hugonnet, R., McNabb, R., Berthier, E., Menounos, B., Nuth, C., Girod, L., et al. (2021). Accelerated global glacier mass loss in the early twenty-first century. *Nature*, *592*, 726–731. https://doi.org/10.1038/s41586-021-03436-z

Huss, M., & Bauder, A. (2009). Twentieth-century climate change inferred from four long-term point observations of seasonal mass balance. *Annals of Glaciology*, *50*(50), 207–214. https://doi.org/10.3189/172756409787769645

Huss, M., Funk, M., & Ohmura, A. (2009). Strong Alpine glacier melt in the 1940s due to enhanced solar radiation. *Geophysical Research Letters*, *36*(23). https://doi.org/10.1029/2009GL040789

Immerzeel, W. W., & Bierkens, M. F. P. (2012). Asia's water balance. *Nature Geoscience*, *5*, 841–842. https://doi.org/10.1038/ngeo1643

Immerzeel, W. W., Lutz, A. F., Andrade, M., Bahl, A., Biemans, H., Bolch, T., et al. (2020). Importance and vulnerability of the world's water towers. *Nature*, *577*(7790), 364–369. https://doi.org/10.1038/s41586-019-1822-y

Immerzeel, W. W., van Beek, L. P. H., & Bierkens, M. F. P. (2010). Climate change will affect the Asian Water Towers. *Science*, *328*, 1382–1385. https://doi.org/10.1126/science.1183188

Jennings, K. S., Winchell, T. S., Livneh, B., & Molotch, N. P. (2018). Spatial variation of the rain-snow temperature threshold across the Northern Hemisphere. *Nature Communications*, *9*(1), 1148. https://doi.org/10.1038/s41467-018-03629-7

Kendall, M. G. (1975). *Rank correlation methods*. London: Griffin.

Kraaijenbrink, P. D. A., Stigter, E. E., Yao, T., & Immerzeel, W. W. (2021). Climate change decisive for Asia's snow meltwater supply. *Nature Climate Change*, *11*, 591–597. https://doi.org/10.1038/s41558-021-01074-x

Lange, S. (2016). *EartH2Observe, WFDEI, and ERA-Interim data Merged and Bias-corrected for ISIMIP (EWEMBI)*. GFZ Data Services. https://doi.org/10.5880/pik.2016.004

Lange, S. (2018). Bias correction of surface downwelling longwave and shortwave radiation for the EWEMBI data set. *Earth System Dynamics*, *9*(2), 627–645. https://doi.org/10.5194/esd-9-627-2018

Lawrence, D. M., Oleson, K. W., Flanner, M. G., Thornton, P. E., Swenson, S. C., Lawrence, P. J., et al. (2011). Parameterization improvements and functional and structural advances in version 4 of the community land model. *Journal of Advances in Modeling Earth Systems*, *3*(1). https://doi.org/10.1029/2011MS00045

Li, S., Yao, T., Yang, W., Yu, W., & Zhu, M. (2018). Glacier energy and mass balance in the Inland Tibetan Plateau: Seasonal and interannual variability in relation to atmospheric changes. *Journal of Geophysical Research: Atmospheres*, *123*(12), 6390–6409. https://doi.org/10.1029/2017JD028120

Li, X., Long, D., Han, Z., Scanlon, B. R., Sun, Z., Han, P., & Hou, A. (2019). Evapotranspiration estimation for Tibetan Plateau headwaters using conjoint terrestrial and atmospheric water balances and multisource remote sensing. *Water Resources Research*, *55*(11), 8608–8630. https://doi.org/10.1029/2019WR025196

Lin, C., Wu, H., Ou, T., & Chen, D. (2019). A new perspective on solar dimming over the Tibetan Plateau. *International Journal of Climatology*, *39*(1), 302–316. https://doi.org/10.1002/joc.5807

Litt, M., Shea, J., Wagnon, P., Steiner, J., Koch, I., Stigter, E., & Immerzeel, W. (2019). Glacier ablation and temperature indexed melt models in the Nepalese Himalaya. *Scientific Reports*, *9*(1), 5264. https://doi.org/10.1038/s41598-019-41657-5

Liu, X., Xu, Z., Yang, H., & Vaghefi, S. (2021). Responses of the glacier mass balance to climate change in the Tibetan Plateau during 1975–2013. *Journal of Geophysical Research: Atmospheres*, *126*(7), e2019JD032132. https://doi.org/10.1029/2019JD032132

Lutz, A. F., Immerzeel, W. W., Shrestha, A. B., & Bierkens, M. F. P. (2014). Consistent increase in High Asia's runoff due to increasing glacier melt and precipitation. *Nature Climate Change*, *4*(7), 587–592. https://doi.org/10.1038/nclimate2237

Makokha, G., Wang, L., Zhou, J., Li, X., Wang, A., Wang, G., & Kuria, D. (2016). Quantitative drought monitoring in a typical cold river basin over Tibetan Plateau: An integration of meteorological, agricultural and hydrological droughts. *Journal of Hydrology*, *543*, 782–795. https://doi.org/10.1016/j.jhydrol.2016.10.050

Mann, H. B. (1945). Nonparametric tests against trend. *Econometrica*, *13*(3), 245–259. https://doi.org/10.2307/1907187

Marzeion, B., Hock, R., Anderson, B., Bliss, A., Champollion, N., Fujita, K., et al. (2020). Partitioning the uncertainty of ensemble projections of global glacier mass change. *Earth's Future*, *8*(7), e2019EF001470. https://doi.org/10.1029/2019EF001470

Miles, E. S., McCarthy, M., Dehecq, A., Kneib, M., Fugger, S., & Pellicciotti, F. (2021). Health and sustainability of glaciers in High Mountain Asia. *Nature Communications*, *12*, 2868. https://doi.org/10.1038/s41467-021-23073-4

Miles, E. S., Willis, I., Buri, P., Steiner, J. F., Arnold, N. S., & Pellicciotti, F. (2018). Surface pond energy absorption across four Himalayan Glaciers accounts for 1/8 of total catchment ice loss. *Geophysical Research Letters*, *45*(19), 10464–10473. https://doi.org/10.1029/2018GL079678

Milly, P. C. D., Dunne, K. A., Milly, P. C. D., & Dunne, K. A. (2020). Colorado River flow dwindles as warming-driven loss of reflective snow energizes evaporation. *Science*, *367*, 1252–1255. https://doi.org/10.1126/science.aay9187

Mölg, T., Maussion, F., & Scherer, D. (2014). Mid-latitude westerlies as a driver of glacier variability in monsoonal High Asia. *Nature Climate Change*, *4*, 68–73. https://doi.org/10.1038/nclimate2055

Mölg, T., Maussion, F., Yang, W., Scherer, D. (2012). The footprint of Asian monsoon dynamics in the mass and energy balance of a Tibetan glacier. *The Cryosphere*, *6*, 1445–1461. https://doi.org/10.5194/tc-6-1445-2012

Nie, Y., Pritchard, H. D., Liu, Q., Hennig, T., Wang, W., Wang, X., et al. (2021). Glacial change and hydrological implications in the Himalaya and Karakoram. *Nature Reviews Earth & Environment*, *2*, 1–106. https://doi.org/10.1038/s43017-020-00124-w

Pritchard, H. D. (2019). Asia's shrinking glaciers protect large populations from drought stress. *Nature*, *569*(7758), 649–654. https://doi.org/10.1038/s41586-019-1240-1

Qi, W., Feng, L., Yang, H., Liu, J., Zheng, Y., Shi, H., et al. (2022). Economic growth dominates rising potential flood risk in the Yangtze River and benefits of raising dikes from 1991 to 2015. *Environmental Research Letters*, *17*, 034046. https://doi.org/10.1088/1748-9326/ac5561

RGI Consortium. (2017). *Randolph Glacier Inventory—A data set of global glacier outlines: Version 6.0: Technical Report, global land ice measurements from space*. Colorado, USA. https://doi.org/10.7265/N5-RGI-60

Scherler, D., Bookhagen, B., & Strecker, M. R. (2011). Spatially variable response of Himalayan glaciers to climate change affected by debris cover. *Nature Geoscience*, *4*(3), 156–159. https://doi.org/10.1038/ngeo1068

Sellers, P. J., Randall, D. A., Collatz, G. J., Berry, J. A., Field, C. B., Dazlich, D. A., et al. (1996). A revised land surface parameterization (SiB2) for atmospheric GCMS. Part I: Model formulation. *Journal of Climate*, *9*(4), 676–705. https://doi.org/10.1175/1520-0442(1996)009<0676:arlspf>2.0.co;2

Sellers, P. J., Tucker, C. J., Collatz, G. J., Los, S. O., Justice, C. O., Dazlich, D. A., & Randall, D. A. (1996). A revised land surface parameterization (SiB2) for atmospheric GCMS. Part II: The generation of global fields of terrestrial biophysical parameters from satellite data. *Journal of Climate*, *9*(4), 706–737. https://doi.org/10.1175/1520-0442(1996)009<0706:arlspf>2.0.co;2

Shean, D. E., Bhushan, S., Montesano, P., Rounce, D. R., Arendt, A., & Osmanoglu, B. (2020). A systematic, regional assessment of High Mountain Asia glacier mass balance. *Frontiers in Earth Science*, *7*, 363. https://doi.org/10.3389/feart.2019.00363

Shen, Y., & Xiong, A. (2016). Validation and comparison of a new gauge-based precipitation analysis over mainland China. *International Journal of Climatology*, *36*(1), 252–265. https://doi.org/10.1002/joc.4341

Shrestha, M., Koike, T., Hirabayashi, Y., Xue, Y., Wang, L., Rasul, G., & Ahmad, B. (2015). Integrated simulation of snow and glacier melt in water and energy balance-based, distributed hydrological modeling framework at Hunza River Basin of Pakistan Karakoram region. *Journal of Geophysical Research: Atmospheres*, *120*(10), 4889–4919. https://doi.org/10.1002/2014JD022666

Shrestha, M., Wang, L., Koike, T., Xue, Y., & Hirabayashi, Y. (2010). Improving the snow physics of WEB-DHM and its point evaluation at the SnowMIP sites. *Hydrology and Earth System Sciences*, *14*(12), 2577–2594. https://doi.org/10.5194/hess-14-2577-2010

Sicart, J., Hock, R., Six, D., (2008). Glacier melt, air temperature, and energy balance in different climates: The Bolivian Tropics, the French Alps, and northern Sweden. *Journal of Geophysical Research: Atmospheres*, *113*(D24). https://doi.org/10.1029/2008JD010406

Su, F., Zhang, L., Ou, T., Chen, D., Yao, T., Tong, K., & Qi, Y. (2016). Hydrological response to future climate changes for the major upstream river basins in the Tibetan Plateau. *Global and Planetary Change*, *136*, 82–95. https://doi.org/10.1016/j.gloplacha.2015.10.012

Thibert, E., Sielenou, D. P., Vionnet, V., Eckert, N., & Vincent, C. (2018). Causes of glacier melt extremes in the Alps since 1949. *Geophysical Research Letters*, *45*(2), 817–825. https://doi.org/10.1002/2017GL076333

Thiery, W., Davin, E. L., Lawrence, D. M., Hirsch, A. L., Hauser, M., & Seneviratne, S. I. (2017). Present-day irrigation mitigates heat extremes. *Journal of Geophysical Research: Atmospheres*, *112*(3), 1403–1422. https://doi.org/10.1002/2016JD025740

van Genuchten, M. T. (1980). A closed form equation for predicting the hydraulic conductivity of unsaturated soils. *Soil Science Society of America Journal*, *44*(5), 892–898. https://doi.org/10.2136/sssaj1980.03615995004400050002x

Vincent, C., & Six, D. (2013). Relative contribution of solar radiation and temperature in enhanced temperature-index melt models from a case study at Glacier de Saint-Sorlin, France. *Annals of Glaciology*, *54*, 11–17. https://doi.org/10.3189/2013AoG63A301

Wang, L., Koike, T., Yang, K., Jackson, T. J., Bindlish, R., & Yang, D. (2009). Development of a distributed biosphere hydrological model and its evaluation with the Southern Great Plains Experiments (SGP97 and SGP99). *Journal of Geophysical Research*, *114*(D8). https://doi.org/10.1029/2008jd010800

Wang, L., Koike, T., Yang, D. W., & Yang, K. (2009). Improving the hydrology of the simple biosphere model 2 and its evaluation within the framework of a distributed hydrological model. *Hydrological Sciences Journal*, *54*(6), 989–1006. https://doi.org/10.1623/hysj.54.6.989

Wang, L., Koike, T., Yang, K., & Yeh, P. J.-F. (2009). Assessment of a distributed biosphere hydrological model against streamflow and MODIS land surface temperature in the upper Tone River Basin. *Journal of Hydrology*, *377*(1–2), 21–34. https://doi.org/10.1016/j.jhydrol.2009.08.005

Wang, L., Sun, L., Shrestha, M., Li, X., Liu, W., Zhou, J., et al. (2016). Improving snow process modeling with satellite-based estimation of near-surface-air-temperature lapse rate. *Journal of Geophysical Research: Atmospheres*, *121*(20), 12005–12012. https://doi.org/10.1002/2016JD025506

Wang, T., Zhao, Y., Xu, C., Ciais, P., Liu, D., Yang, H., et al. (2021). Atmospheric dynamic constraints on Tibetan Plateau freshwater under Paris climate targets. *Nature Climate Change*, *11*, 1–225. https://doi.org/10.1038/s41558-020-00974-8

Wang, L., Zhou, J., Qi, J., Sun, L., Yang, K., Tian, L., et al. (2017). Development of a land surface model with coupled snow and frozen soil physics. *Water Resources Research*, *53*(6), 5085–5103. https://doi.org/10.1002/2017WR020451

Wijngaard, R. R., Steiner, J. F., Kraaijenbrink, P. D. A., Klug, C., Adhikari, S., Banerjee, A., et al. (2019). Modeling the response of the Langtang Glacier and the Hintereisferner to a changing climate since the Little Ice Age. *Frontiers in Earth Science*, *7*. https://doi.org/10.3389/feart.2019.00143

Woolway, I. R., Jennings, E., Shatwell, T., Golub, M., Pierson, D. C., & Maberly, S. C. (2021). Lake heatwaves under climate change. *Nature*, *589*, 402–407. https://doi.org/10.1038/s41586-020-03119-1

Yang, D. (1998). *Distributed hydrological model using hillslope discretization based on catchment area function: Development and applications, (Ph.D.)*. University of Tokyo.

Yang, K., Ding, B., Qin, J., Tang, W., Lu, N., & Lin, C. (2012). Can aerosol loading explain the solar dimming over the Tibetan Plateau? *Geophysical Research Letters*, *39*(20), L20710. https://doi.org/10.1029/2012GL053733

Yang, W., Guo, X., Yao, T., Yang, K., Zhao, L., Li, S., & Zhu, M. (2011). Summertime surface energy budget and ablation modeling in the ablation zone of a maritime Tibetan glacier. *Journal of Geophysical Research: Atmospheres*, *116*(D14). https://doi.org/10.1029/2010JD015183

Yang, W., Yao, T., Guo, X., Zhu, M., Li, S., & Kattel, D. B. (2013). Mass balance of a maritime glacier on the southeast Tibetan Plateau and its climatic sensitivity. *Journal of Geophysical Research: Atmospheres*, *118*(17), 9579–9594. https://doi.org/10.1002/jgrd.50760

Yao, T., Xue, Y., Chen, D., Chen, F., Thompson, L., Cui, P., et al. (2019). Recent Third Pole's rapid warming accompanies cryospheric melt and water cycle intensification and interactions between monsoon and environment: Multi-disciplinary approach with observation, modeling, and analysis. *Bulletin of the American Meteorological Society*, *100*(3), 423–444. https://doi.org/10.1175/BAMS-D-17-0057.1

You, Q., Kang, S., Flügel, W.-A., Sanchez-Lorenzo, A., Yan, Y., Huang, J., & Martin-Vide, J. (2009). From brightening to dimming in sunshine duration over the eastern and central Tibetan Plateau (1961–2005). *Theoretical and Applied Climatology*, *101*, 445–457. https://doi.org/10.1007/s00704-009-0231-9

Zemp, M., Huss, M., Thibert, E., Eckert, N., McNabb, R., Huber, J., et al. (2019). Global glacier mass changes and their contributions to sea-level rise from 1961 to 2016. *Nature*, *568*(7752), 382–386. https://doi.org/10.1038/s41586-019-1071-0

Zhang, L., Su, F., Yang, D., Hao, Z., & Tong, K. (2013). Discharge regime and simulation for the upstream of major rivers over Tibetan Plateau. *Journal of Geophysical Research: Atmospheres*, *118*(15), 8500–8518. https://doi.org/10.1002/jgrd.50665

Zhang, Y., Hao, Z., Xu, C.-Y., & Lai, X. (2019). Response of melt water and rainfall runoff to climate change and their roles in controlling streamflow changes of the two upstream basins over the Tibetan Plateau. *Hydrology Research*, *51*(2), 272–289. https://doi.org/10.2166/nh.2019.075

Zhao, Y., & Zhu, J. (2015). Assessing quality of grid daily precipitation data sets in China in recent 50 yr (in Chinese). *Plateau Meteorology*, *34*(1), 50–58

Zhou, J., Wang, L., Zhang, Y., Guo, Y., Li, X., & Liu, W. (2015). Exploring the water storage changes in the largest lake (Selin Co) over the Tibetan Plateau during 2003–2012 from a basin-wide hydrological modeling. *Water Resources Research*, *51*(10), 8060–8086. https://doi.org/10.1002/2014WR015846

Zhu, M., Yao, T., Yang, W., Maussion, F., Huintjes, E., & Li, S. (2015). Energy-and mass-balance comparison between Zhadang and Parlung No. 4 glaciers on the Tibetan Plateau. *Journal of Glaciology*, *61*(227), 595–607. https://doi.org/10.3189/2015JoG14J206

Zhu, M., Yao, T., Yang, W., Xu, B., Wu, G., & Wang, X. (2018). Differences in mass balance behavior for three glaciers from different climatic regions on the Tibetan Plateau. *Climate Dynamics*, *50*, 3457–3484. https://doi.org/10.1007/s00382-017-3817-4

References From the Supporting Information

Dee, D. P., Uppala, S. M., Simmons, A. J., Berrisford, P., Poli, P., Kobayashi, S., et al. (2011). The ERA-Interim reanalysis: Configuration and performance of the data assimilation system. *Quarterly Journal of the Royal Meteorological Society*, *137*(656), 553–597. https://doi.org/10.1002/qj.828

Hempel, S., Frieler, K., Warszawski, L., Schewe, J., Piontek, F. (2013). A trend-preserving bias correction—The ISI-MIP approach. *Earth System Dynamics*, *4*(2): 219–236. https://doi.org/10.5194/esd-4-219-2013

People's Republic of China. (2008). *Standard for hydrological information and hydrological forecasting*(p. 10). Beijing: China Standards Press.

Qi, W., Liu, J., & Chen, D. (2018). Evaluations and improvements of GLDAS2.0 and GLDAS2.1 forcing data's applicability for basin scale hydrological simulations in the Tibetan Plateau. *Journal of Geophysical Research: Atmospheres*, *123*(23), 13128–13148. https://doi.org/10.1029/2018JD029116

Qi, W., Liu, J., Xia, J., & Chen, D. (2020). Divergent sensitivity of surface water and energy variables to precipitation product uncertainty in the Tibetan Plateau. *Journal of Hydrology*, *581*, 124338. https://doi.org/10.1016/j.jhydrol.2019.124338

Qi, W., Zhang, C., Fu, G., & Zhou, H. (2016). Quantifying dynamic sensitivity of optimization algorithm parameters to improve hydrological model calibration. *Journal of Hydrology*, *533*, 213–223. https://doi.org/10.1016/j.jhydrol.2015.11.052

Rabus, B., Eineder, M., Roth, A., & Bamler, R. (2003). The shuttle radar topography mission—A new class of digital elevation models acquired by spaceborne radar. *ISPRS Journal of Photogrammetry and Remote Sensing*, *57*(4), 241–262. https://doi.org/10.1016/s0924-2716(02)00124-7

Schellekens, J., Dutra, E., laTorre, A., Balsamo, G., van Dijk, A., Weiland, F., et al. (2017). A global water resources ensemble of hydrological models: The eartH2Observe Tier-1 data set. *Earth System Science Data*, *9*(2), 389–413. https://doi.org/10.5194/essd-9-389-2017

Tolson, B. A., Asadzadeh, M., Maier, H. R., & Zecchin, A. (2009). Hybrid discrete dynamically dimensioned search (HD-DDS) algorithm for water distribution system design optimization. *Water Resources Research*, *45*(12), W12416. https://doi.org/10.1029/2008WR007673

Tolson, B. A., & Shoemaker, C. A. (2008). Efficient prediction uncertainty approximation in the calibration of environmental simulation models. *Water Resources Research*, *44*(4), W04411. https://doi.org/10.1029/2007wr005869

Zhu, Z., Bi, J., Pan, Y., Ganguly, S., Anav, A., Xu, L., et al. (2013). Global data sets of vegetation leaf area index (LAI)3g and fraction of photosynthetically active radiation (FPAR)3g derived from Global Inventory Modeling and Mapping Studies (GIMMS) normalized difference vegetation index (NDVI3g) for the period 1981–2011. *Remote Sensing*, *5*(2), 927–948. https://doi.org/10.3390/rs5020927